Typeset with jpsj2.cls <ver.1.1.1>

arXiv:cond-mat/0607368v1 [cond-mat.supr-con] 14 Jul 2006

In-plane Anisotropy of the Magnetic Fluctuations in $Na_xCoO_2 \cdot yH_2O$

C. Michioka, Y. Itoh, H. Ohta, M. Kato[1] and K. Yoshimura

Department of Chemistry, Graduate School of Science,
Kyoto University, Kyoto 606-8502, Japan
[1]*Department of Molecular Science and Technology, Faculty of Engineering,*
Doshisha University, Kyotanabe, Kyoto 610-0394, Japan

(Received February 6, 2008)

We report the ^{59}Co NMR studies of the in-plane anisotropy of bilayer hydrated $Na_xCoO_2 \cdot yH_2O$ using a oriented powder sample by a magnetic field in Fluorinert FC70. We found for the first time the *ab*-plane anisotropy of the ^{59}Co NMR Knight shift K, the nuclear spin-lattice relaxation rate $1/T_1$ and the nuclear spin-spin relaxation rate $1/T_2$ at a magnetic field $H \sim 7.5$ T up to 200K. Below 75 K, the anisotropy of K is large compared with that at high temperatures. The hyperfine coupling constants seem to change around the temperature 150 K, in which the bulk susceptibility χ shows broad minimum, suggesting a change of the electronic state of CoO_2 plane. $1/T_1$ also shows a significant anisotropy, which cannot be explained only by the anisotropy of the hyperfine coupling constants nor the anisotropic uniform spin susceptibility. The difference in the in-plane anisotropy of T_1 from that of K indicates that the magnetic fluctuation at a finite wave vector $\vec{q} \neq 0$ is also anisotropic and the anisotropy is different from that at $\vec{q} = 0$.

KEYWORDS: superconductivity, sodium cobalt oxide, NMR, anisotropy

Since the discovery of the superconductivity on the triangular CoO_2 plane in $Na_xCoO_2 \cdot yH_2O$,[1)] not only the superconducting state but also the normal state have been intensively studied to understand the unique properties and the electronic structure. In contrast to the high-T_c cuprate, in the case of cobaltate it is necessary to consider a t_{2g}-orbital magnetism of Co^{4+} (d^5). Sodium deficiencies and oxonium ions introduce a mixing state of $S = 0$ Co^{3+} and $S = 1/2$ Co^{4+}. The CoO_2 layers in $Na_xCoO_2 \cdot yH_2O$ consist of edge shared CoO_6 octahedra which are compressed along the trigonal axis. The trigonal distortion and spin-orbit interaction divide the t_{2g} level into three levels (the f, g, and h states labeled in Ref. [2]). In Co^{4+}, a hole with pseudospin 1/2 resides on the f level, whose wave function contains both e'_g ($|l_z = \pm 1\rangle$) and a_{1g} ($|l_z = 0\rangle$) states mixed up by a spin-orbit coupling.[2)] Although the orbital moment can give an anisotropy to the magnetic moment even in the itinerant system, the microscopic and macroscopic details of in-plane magnetic anisotropy in $Na_xCoO_2 \cdot yH_2O$ remain to be explored so far.

Due to the nature of the soft chemical treatment, it is difficult to intercalate the water molecules homogeneously into Na_xCoO_2 to prepare a bilayer hydrated sample, especially in a large single crystal. Therefore, in the present stage, the bilayer hydrated powder samples are still more homogeneous than single crystals and reliable to study the intrinsic physical properties. In the previous work, we observed the two-dimensional (2D) powder pattern of ^{59}Co NMR by using an organic solvent hexane to fix the powders under a magnetic field of 8 T.[3)] However, hexane is not convenient due to a volatile property and then we could not obtain the higher temperature data. We need a convenient solvent, which does not absorb water molecules and have an appropriate melting point. Recently, we found that Fluorinert is most suitable for fixing powders of $Na_xCoO_2 \cdot yH_2O$ and we succeeded in measuring the well-oriented 2D powder data up to 200K.

In this paper, we report for the first time the *ab*-plane anisotropy of the ^{59}Co NMR Knight shift K, the nuclear spin-lattice relaxation rate $1/T_1$ and the nuclear spin-spin relaxation rate $1/T_2$ at a magnetic field $H \sim 7.5$ T up to 200 K for the bilayer hydrated $Na_xCoO_2 \cdot yH_2O$ with $T_c = 4.8$ K. We found that K_x strongly depends on temperature while K_y increases slightly with the decrease of temperature. We also obtained the striking result that $1/T_1$ at $H \parallel x$-axis is about two times larger than that at $H \parallel y$-axis. The T_1 anisotropy cannot be explained only by the anisotropic hyperfine coupling constants.

The ^{59}Co NMR and nuclear quadrupole resonance (NQR) were carried out for the optimal $T_c = 4.8$ K sample of bilayer hydrated $Na_xCoO_2 \cdot yH_2O$, which gives a optimal superconductivity in the phase diagram.[4,5)] The powders of $Na_xCoO_2 \cdot yH_2O$ were oriented under a magnetic field of $H \sim 7.5$ T by Fluorinert FC70 (melting point of 248 K). In this situation, the c-axis is oriented perpendicular to the external field and the c-plane is oriented randomly along the magnetic field. All the frequency-swept ^{59}Co NMR spectra at the center resonance ($I_z = -1/2 \leftrightarrow +1/2$) were measured under a magnetic field of 7.4847 T with a conventional spin-echo technique. The ^{59}Co nuclear spin-lattice relaxation time $^{59}T_1$ was measured by an inversion recovery technique. The spin-echo signal $M(t)$ was measured as a function of long delay time t after an inversion pulse, and $M(\infty)[\equiv M(t > 10T_1)]$ was recorded. The nuclear spin-spin relaxation time $^{59}T_2$ was measured by the spin-echo decay.

Figure 1 shows the 2D powder ^{59}Co NMR spectra between 10 and 200 K. These resonance lines arise from the transition, $I_z = \pm 5/2 \leftrightarrow \pm 7/2$ of ^{59}Co (nuclear spin $I = 7/2$). In all data, the spin-echo intensities at the

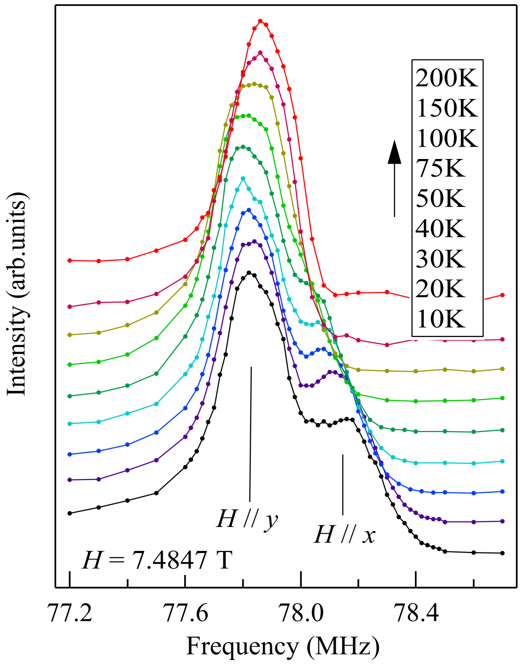

Fig. 1. Center lines ($I_z = -1/2 \leftrightarrow +1/2$) of the frequency-swept ^{59}Co NMR spectra in Na$_x$CoO$_2$$\cdot$$yH_2$O under a magnetic field of 7.4847 T. Two-peak structure is explained by the anisotropic Knight shifts but not the asymmetry parameter η.

frequencies far from the resonance center are close to zero, suggesting in-plane well-oriented 2D powder spectra. The spectrum at 10 K shows a two-peak structure, which is explained by a lower symmetric spectrum than a uniaxial symmetry.$^{3)}$ The peaks at lower and higher frequencies correspond to $H \parallel y$ and $H \parallel x$, respectively. Although the effect of a non-uniaxial electric field gradient with a finite asymmetry parameter η would split the resonance peak, the large splitting of the observed spectrum cannot be explained by η which is estimated by the NQR measurement (see below). The temperature dependence of the peak frequencies is mainly due to the temperature dependence of the Knight shifts but not the quadrupole shift. The peak frequency of K_y slightly decreases with increasing temperature, while that of K_x decreases markedly. The K_y and K_x peaks can be clearly distinguishable below 75 K. At 100 and 150 K, the K_y and K_x peaks are not clearly split, suggesting that K_y is similar to K_x. At 200 K, the spectrum can be fitted by a double Gaussian function.

In order to estimate quantitatively the quadrupole shift and decide the intrinsic Knight shift, we carried out the ^{59}Co NQR measurements. Figure 2(a) shows the ^{59}Co NQR spectra between 10 and 200 K. The lower and higher frequency peaks in the NQR spectra correspond to the resonances $I_z = \pm 3/2 \leftrightarrow \pm 5/2$, ν_2 and $I_z = \pm 5/2 \leftrightarrow \pm 7/2$, ν_3, respectively. We estimated a quadrupole resonance frequency $\nu_{\rm Q}$ and an asymmetric parameter $\eta \equiv (\partial^2 V/\partial x^2 - \partial^2 V/\partial y^2)/(\partial^2 V/\partial z^2)$ from ν_2 and ν_3.$^{6)}$ The nuclear spin Hamiltonian of the quadrupole interaction is expressed as

$$H_Q = a[3I_z^2 - I(I+1) + \frac{1}{2}\eta(I_+^2 + I_-^2)], \qquad (1)$$

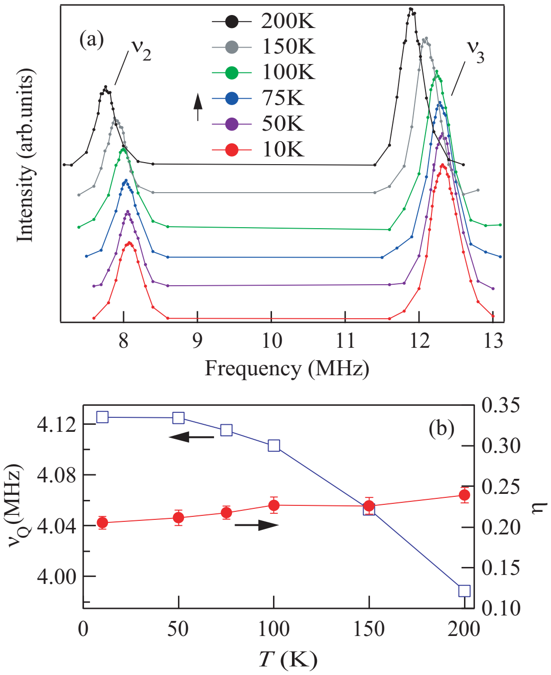

Fig. 2. (a) Temperature dependence of ^{59}Co NQR spectra. Lower and higher frequency peaks correspond to ν_2 ($I_z = \pm 3/2 \leftrightarrow \pm 5/2$) and ν_3 ($I_z = \pm 5/2 \leftrightarrow \pm 7/2$), respectively. (b) Temperature dependence of $\nu_{\rm Q}$ and η are calculated from the ν_2 and ν_3.

$$a = \frac{e^2 qQ}{4I(2I-1)} = \frac{\nu_{\rm Q} h}{6}. \qquad (2)$$

Then the eigen value equation for $I = 7/2$ is written as

$$E^4 - 42(1 + \frac{1}{3}\eta^2)(3a)^2 E^2 - 64(1-\eta^2)(3a)^3 E + 105(1 + \frac{1}{3}\eta^2)^2(3a)^4 = 0. \qquad (3)$$

The eigen values of four Kramers doublets ($E_{\pm 7/2}$, $E_{\pm 5/2}$, $E_{\pm 3/2}$, $E_{\pm 1/2}$) were numerically solved. Then we obtained $\nu_3 \equiv E_{\pm 7/2} - E_{\pm 5/2}$ and $\nu_2 \equiv E_{\pm 5/2} - E_{\pm 3/2}$ as functions of $\nu_{\rm Q}$ and η. η was determined from the ratio of ν_2/ν_3, and then the quaqrapole frequency $\nu_{\rm Q}$ was estimated from η and ν_3. The obtained $\nu_{\rm Q}$ and η are shown in Fig. 2(b). $\nu_{\rm Q}$ is almost invariant between 10 and 50 K and decreases as temperature increases up to 200 K, while η increases slightly.

Figure 3(a) shows the temperature dependence of the Knight shifts determined by using the NQR parameters and second-order perturbation theory.$^{3)}$ As mentioned above, the two peaks of the spectra are mainly due to the in-plane anisotropy of the Knight shift but not that of the quadrupole shift. From the analysis of the shape of NMR spectra, at 100 and 150 K the Knight shifts are almost isotropic in the ab-plane and once again slightly anisotropic at 200 K. Below 100K, the distinguishable two-peak structure of NMR spectra can be explained by the ab-plane anisotropic Knight shifts K_x and K_y. K_x increases monotonically with decreasing temperature, while K_y slightly increases. Thus, it turned out that the low temperature Curie-Weiss-type upturn of the magnetic susceptibility$^{3)}$ is intrinsic.

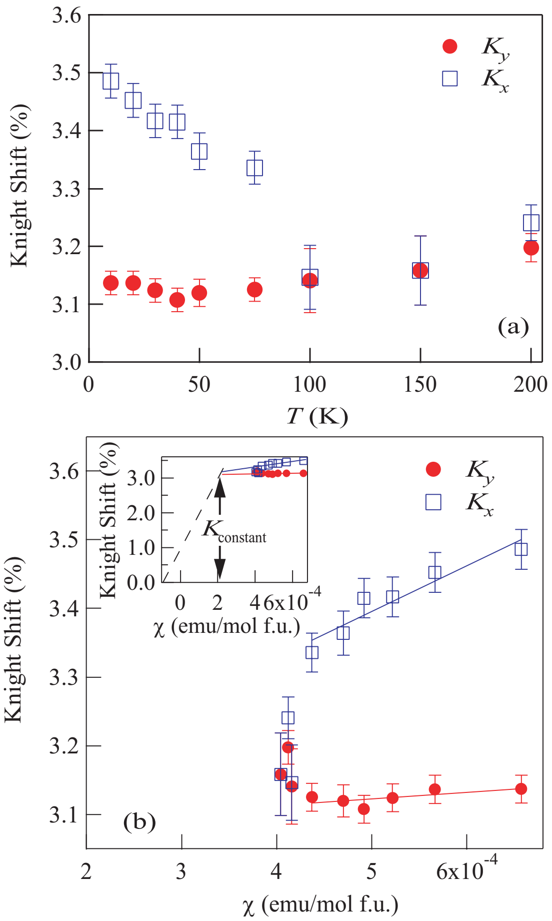

Fig. 3. (a) ^{59}Co Knight shifts K_x and K_y of $Na_xCoO_2{\cdot}yH_2O$. The shifts were estimated with taking account of the quadrupole shift. (b) K-χ plot. The bulk susceptibility χ of powder sample was used as a horizontal axis.

Figure 3(b) is the K-χ plot, where temperature is an implicit parameter. In this plot, we tentatively employ the bulk magnetic susceptibility χ of powder sample. We believe that χ is anisotropic, especially in ab-plane at low temperatures. Below the room temperature, the bulk susceptibility χ decreases with the decrease of temperature and shows a broad minimum around 150 K and again increases down to 10 K. Since the two peaks corresponding to $H \parallel x$ and $H \parallel y$ are obviously distinguishable and the two distinct lines are held below 75 K, we can estimate the hyperfine coupling constants as $A_x = +37.2$ kOe/μ_B and $A_y = +5.2$ kOe/μ_B, respectively, from the data below 75 K. The value of A_x is similar to that previously estimated while A_y is less than half.$^{3)}$ The differences between the present and the previous$^{3)}$ works are mainly due to the imperfect orientation by a magnetic field in the previous work.

Above 100 K, K_x is close to K_y. The linear relations in the K-χ plot do not seem to hold above 100 K. Thus, we can conclude that the hyperfine coupling constants at high temperatures are different from that at low temperatures. Then, the electronic state at the cobalt site is thought to be changed at about the temperature ∼ 150 K, where the bulk χ shows the minimum behavior. The change may be attributed in a motion of sodium ions or a tendency of superlattice formation. The anomalies found in $1/T_1$ of the ^{23}Na NMR implies a sodium contribution to the change of the electronic state in the CoO_2 plane.$^{7)}$ As shown in the inset figure, a temperature independent Knight shift, which consists of contributions of the diamagnetism, the orbital part and maybe a temperature-independent spin part, is estimated about 3 %. The detailed analysis has already been reported.$^{3)}$

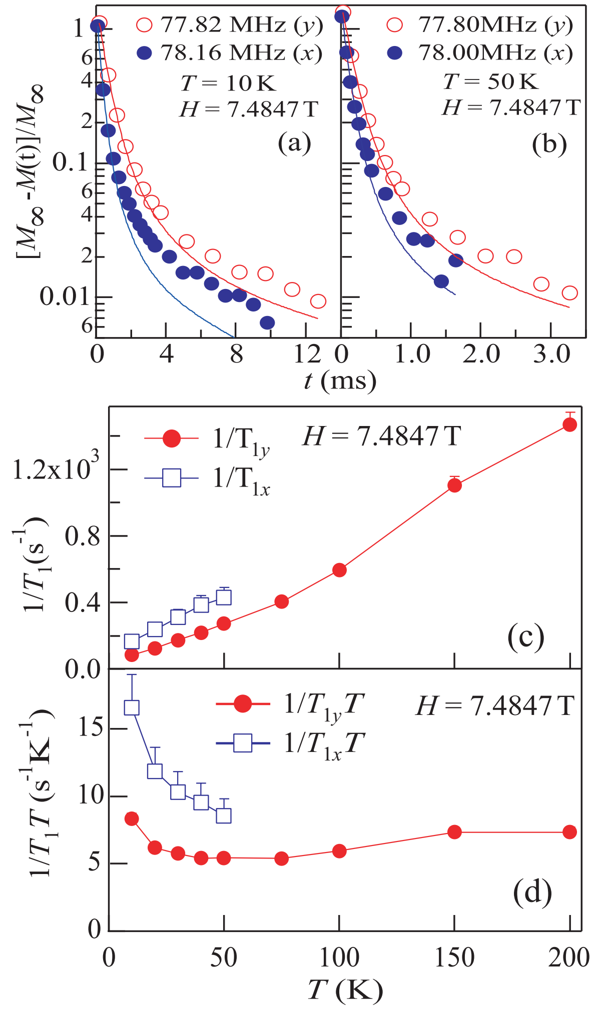

Fig. 4. Recovery curves at (a) 10 and (b) 50 K. Open and closed circles represent the data measured at the peak frequencies of K_y and K_x, respectively. Solid lines are fitted lines by the theoretical relaxation function. Temperature dependence of (c) $1/T_1$ and (d) $1/T_1T$.

Figures 4(a) and (b) show the ^{59}Co nuclear spin-echo recovery curves at $H \parallel y$-axis (lower frequency) and at $H \parallel x$-axis (higher frequency) at 10 and 50 K, respectively. The recovery curves were fitted by the theoretical relaxation function of the central resonance, as follows:

$$\frac{M(\infty) - M(t)}{M(\infty)}$$
$$= M_0 \left(\frac{1}{84} e^{\frac{-t}{T_1}} + \frac{3}{44} e^{\frac{-6t}{T_1}} + \frac{75}{364} e^{\frac{-15t}{T_1}} + \frac{1225}{1716} e^{\frac{-28t}{T_1}} \right), \tag{4}$$

where M_0 and T_1 are fitting parameters. The obtained recovery curves at the peak-frequency of K_y agree with theoretical curves. However, a small slow component at

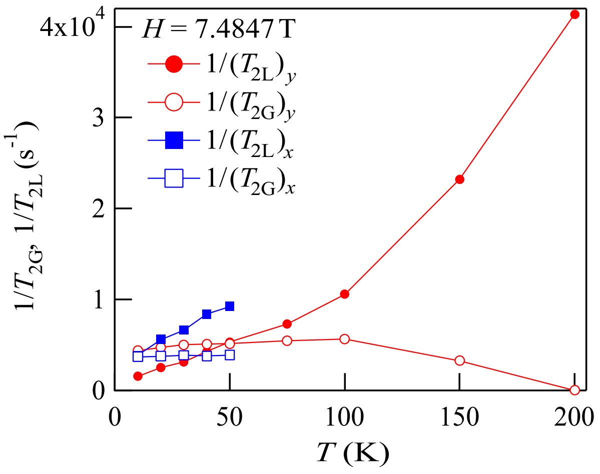

Fig. 5. Temperature dependence of $1/(T_{2G})_i$ and $1/(T_{2L})_i$ ($i = x, y$).

K_x exists maybe due to a small contribution of K_y, and then the experimental curves were fitted by the theoretical curves up to 1/10 decay. One can find obvious differences in recovery curves at $H \parallel y$ and at $H \parallel x$.

Figure 4(c) shows the temperature dependence of the nuclear spin-lattice relaxation rate at the peak frequencies of $H \parallel y$, $1/T_{1y}$ and that of $H \parallel x$, $1/T_{1x}$. Figure 4(d) shows $1/T_{1i}T$ ($i = x, y$). The temperature dependence of $1/T_{1y}$ is similar to that at $H = 0$ T, which was measured by NQR,[3] however, the absolute values are smaller, suggesting the suppression of the magnetic fluctuations by the magnetic field. $1/T_{1x}$ is clearly different from $1/T_{1y}$ below 50 K.

In Fig. 4(d), we obtained the significant result that $1/T_{1x}T$ is about two times larger than $1/T_{1y}T$. Since $1/T_{1i}$ ($i = x, y$) should arise from the magnetic fluctuations $(\delta h)^2$ perpendicular to the i direction, $1/T_{1x}$ and $1/T_{1y}$ should be proportional to $(\delta h_z)^2 + (\delta h_y)^2$ and $(\delta h_z)^2 + (\delta h_x)^2$, respectively.[8] $(\delta h_i)^2$ ($i = x, y, z$) is the square of local magnetic field fluctuations along the i-axis. Then the Knight shifts should be $K_x^s = A_x \chi_x$ and $K_y^s = A_y \chi_y$. $1/T_{1x}$ is about two times larger than $1/T_{1y}$, while K_y is smaller than K_x. Therefore, the anisotropy of T_1 cannot be explained only by the anisotropy of the hyperfine coupling constants nor the anisotropic uniform spin susceptibility. The difference in the in-plane anisotropy of T_1 from that of K indicates that the magnetic fluctuation at a finite wave vector $\vec{q} \neq 0$ is also anisotropic and the anisotropy is different from that at $\vec{q} = 0$.

Figure 5 shows the temperature dependence of the transverse relaxation rates of a Gaussian component $1/(T_{2G})_i$ and a Lorentzian component $1/(T_{2L})_i$ ($i = x, y$). Behaviors of $1/(T_{2G})_i$ and $1/(T_{2L})_i$ are similar to that of the nonsuperconducting bilayer hydrated $Na_xCoO_2 \cdot yH_2O$ in NQR measurement.[5] As well as $1/T_1$, especially $1/(T_{2L})_i$ shows a strong anisotropy for x and y. Therefore, the primary contribution to $1/(T_{2L})_i$ is a T_1 process and $1/(T_{2G})_i$ is nuclear spin-spin relaxation rate. At high temperatures, the $1/(T_{2G})_i$ contribution becomes quite small and a part of the transverse relaxation may be originated in a contribution of the sodium motion.

The magnetic susceptibility measured on the single crystal was found to be anisotropic in H parallel and perpendicular to the CoO_2 plane.[9] However, the in-plane anisotropy is not reported. From the temperature-dependent anisotropy of K and $1/T_1$ of the ^{59}Co NMR as well as the anomalous behaviors of the ^{23}Na NMR[7] and the electrical resistivity,[10] one may conclude that the electronic state of CoO_2 plane is different at low and high temperatures, which may be due to the change of the charge-transfer state from sodium and oxonium ions. Unquenched orbital moments may play a significant role in the low temperature state. Unconventional electronic states such as hidden Kagomé symmetry in the CoO_2 plane[11] were proposed from the study of the t_{2g} degeneracy. A variety of the superconducting properties was also studied by taking account of the spin-orbit coupling.[2, 12] The presence of the ab-plane anisotropy of the magnetic fluctuations is a key to reveal the superconducting mechanism in $Na_xCoO_2 \cdot yH_2O$.

This work is supported by Grant-in Aid for Scientific Research on Priority Area "Invention of anomalous quantum materials", from the Ministry of Education, Culture, Sports, Science and Technology of Japan (Grant No. 16076210).

1) K. Takada, H. Sakurai, E. Takayama-Muromachi, F. Izumi, R. A. Dilanian and T. Sasaki: Nature **422** (2003) 53.
2) G. Khaliullin, W. Koshibae and S. Maekawa: Phys. Rev. Lett. **93** (2004) 176401.
3) M. Kato, C. Michioka, T. Waki, Y. Itoh, K. Yoshimura, K. Ishida, K. Takada, H. Sakurai, E. Takayama-Muromachi and T. Sasaki: J. Phys.: Condens. Matter **18** (2006) 669.
4) Y. Ihara, K. Ishida, C. Michioka, M. Kato, K. Yoshimura, K. Takada, T. Sasaki, H. Sakurai and E. Takayama-Muromachi: J. Phys. Soc. Jpn. **74** (2005) 867.
5) C. Michioka, H. Ohta, Y. Itoh and K. Yoshimura: J. Phys. Soc. Jpn. **75** (2006) 063701.
6) A. Abragam: The Principles of Nuclear Magnetism (Oxfird University Press, Oxford, 1961).
7) H. Ohta, C. Michioka, Y. Itoh, K. Yoshimura, H. Sakurai, E. Takayama-Muromachi, K. Takada and T. Sasaki: Physica B **378** (2006) 859; H. Ohta, Y. Itoh, C. Michioka and K. Yoshimura: cond-mat/0508197.
8) T. Moriya: Prog. Theor. Phys. **16** (1956) 23 and 641; T. Moriya: Prog. Theor. Phys. **28** (1962) 371; T. Moriya: J. Phys. Soc. Jpn. **18** (1963) 516.
9) F. C. Chou, J. H. Cho, P. A. Lee, E. T. Abel, K. Matan and Y. S. Lee: Phys. Rev. Lett. **92** (2004) 157004.
10) R. Jin, B. C. Sales, P. Khalifah and D. Mandrus: Phys. Rev. Lett. **91** (2003) 217001.
11) W. Koshibae and S. Maekawa: Phys. Rev. Lett. **91** (2003) 257003.
12) Y. Yanase, M. Mochizuki and M. Ogata: J. Phys. Soc. Jpn. **74** (2005) 3351.